THERMAL MODELING OF RING-TYPE DEFECTS

Yi Xie, Matthias Liepe, David Meidlinger, Hasan Padamsee
Cornell Laboratory for Accelerator-Based Sciences and Education,
Cornell University (CLASSE), Ithaca, NY 14853, USA

Abstract

Thermometry and optical inspection results suggest that pit-like structures in the high magnetic field region of an SRF cavity are possbile defect candidates that cause cavity quench. Previous thermal modeling of pit-like structures based on a disk-type defect model suggests that the observed pit is much larger than the actual normal conducting region responsible for initiating the quench. Guided by the magnetic enhancement calculations of pits, a ring-type defect could be a better model for quench caused by the sharp boundary segment of a pure niobium pit. The relationship between quench field and inner radius of a ring-type defect is presented based on calculations of an improved ring-type defect model.

Figure 1: SEM image of a quench causing pit-like defect found in the cavity LE1-HOR.

INTRODUCTION

The maximum field achieved by superconducting rf cavities is limited by the thermal breakdown initiated from so-called "defect" areas in the high magnetic field region around the equatorial welding zone. Optical inspection techniques found that many of these defect regions can be categorized as pit-like structures [1]. Although most of the pits found did not cause quench at the magnetic field achieved, some of them are responsible for initiaing quench. This indicates that sizes, depth and edge sharpness of the pits may determine the quench onset field. Previous thermal modeling of pit-like structures based on a disk-type defect model suggest that the observed pit is much larger than the actual normal conducting region causing quench [2]. Figure 1 shows an actuall pit which causes a cavity quench at maximum cavity surface magnetic field 1200Oe with its diameter of nearly 1mm. Calculations of the magnetic field enhancement at pits and bumps on the surface of superconducting cavities show that the field enhancement factor for pits can reach the value of 4 depending on the slope of the edge [3]. Figure 2 shows the relative high current density distribution calculated by Microwave Studio$^{@}$ at the edge of a pit structure modeled as a hole on the axis of a pill-box cavity. This indicates that the edge of a pit or a part of it can become normal conducting due to the strong magnetic field enhancement. In order to study the quench initiated from such a ring-shaped normal conducting region at the edge of a niobium pit, a ring-type defect thermal model was developed. Due to the axi- symmetric mesh configurations in the thermal model, arc-type defect model can not be simulated currently.
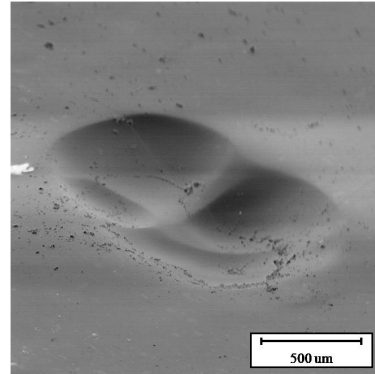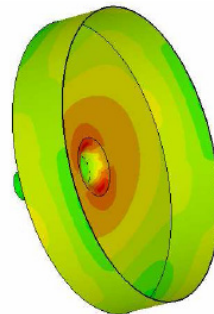

Figure 2: Current density distribution on a pit presented as a hole on the axis of a pill-box cavity. [3]

THERMAL MODELING AND CODE BENCHMARK

The 2-d ring-defect thermal program was developed from a disk-defect thermal program. Heat balance equations and boundary conditions are the same as they were used in a disk-defect model [2]. Figure 3 shows the mesh configuration difference between a ring-type defect and a disk-type defect. For a ring-type defect, the program splits a cylindrical section of the niobium wall into many circular ring-shaped mesh elements. The normal conducting defect is located in a ring section located at a certain distance to the center of the entire modeled niobium disk. Given the temperature dependent thermal conductivity of niobium and Kapitza conductance between niobium and helium, r.f. power produced at the surface is compared with power emitted into the helium bath at a given iteration number. The over-relaxation method is used to estimate the $(n+1)$-th iteration from n-th iteration. Once the two heat transfer

05 Cavity performance limiting mechanisms

numbers are sufficiently equal (e.g. their difference is less than 0.01%), thermal equilibrium is reached. For initial studies, the defect resistance was taken as $10\text{m}\Omega$ which is assumed as the normal resistance of niobium. The real normal conducting surface resistance of a given niobium pit edge does depend on temperature, and therefore the defect region may have a large range of resistances ($1 \sim 10\text{m}\Omega$). To speed up simulations, the mesh density is high near the defect element and lower away from it where temperature gradient are smaller. The mesh spacing in the radial direction was chosen to increase exponentially (the distance between the i-th element to the ring-defect is proportional to $exp(i)$). The z direction is also meshed using an exponential function. Figure 4 is shown to verify that the calculated results are independent of the different mesh density configurations. It shows that the results obtained from the thermal model become independent of the mesh density for sufficiently dense meshes.

Figure 4: rf surface temperature distribution along radial direction for a given shape ring-type defect with different mesh densities

(a) Mesh configuration for a disk-type defect

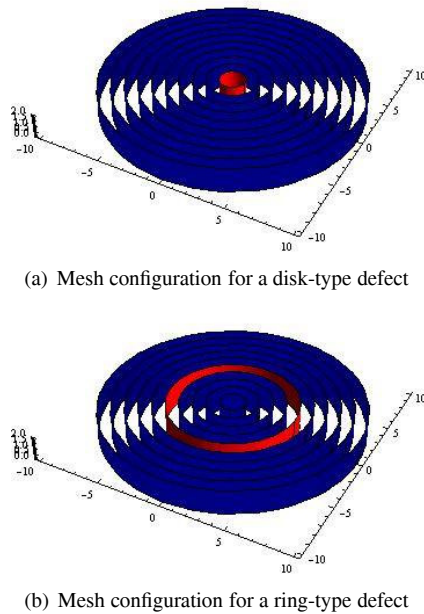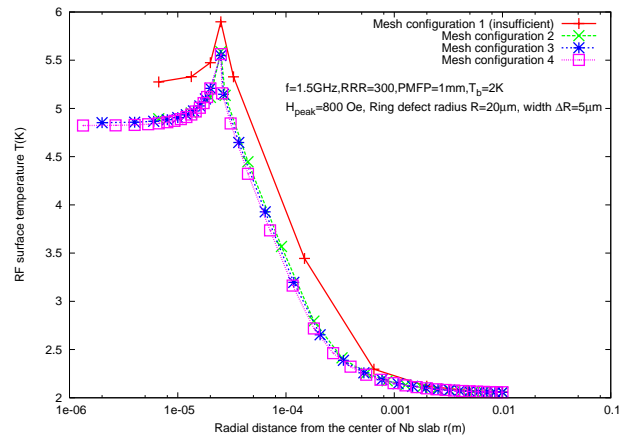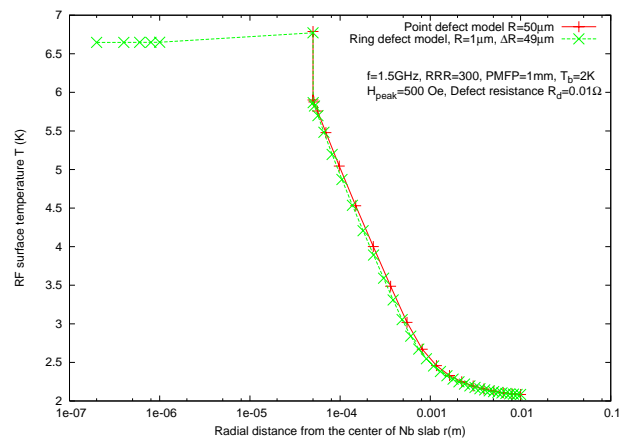(b) Mesh configuration for a ring-type defect

Figure 3: Different mesh distributions of ring-type and disk-type defect models with normal conducting (red) and superconducting (blue) mesh elements.

To test the ring-shape defect thermal modeling program, we have calculated the heating due to a ring-type defect and a disk defect. The ring defect inner radius is 1μm with a ring width of 49μm and the disk defect radius 50μm. The temperature distribution of those two cases should approximately be the same because the rf deposited power in both cases was is nearly equal. Figure 5 shows that the calculated temperature distribution agrees very well indeed for the two cases. In a second test of the program, a large ring-type defect with an inner radius 5mm and ring width 1μm. The result of this simulation is shown in Figure 6. The ring induced heat distribution is nearly symmetric as expected.

Figure 5: rf surface temperature distribution of a disk defect (radius 50 = μm) and of a ring defect (outer radius = 50μm, inner radius = 1μm). The rf deposited power is the same in both cases
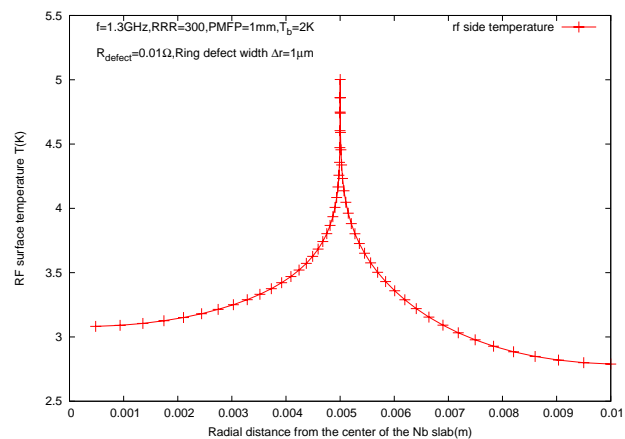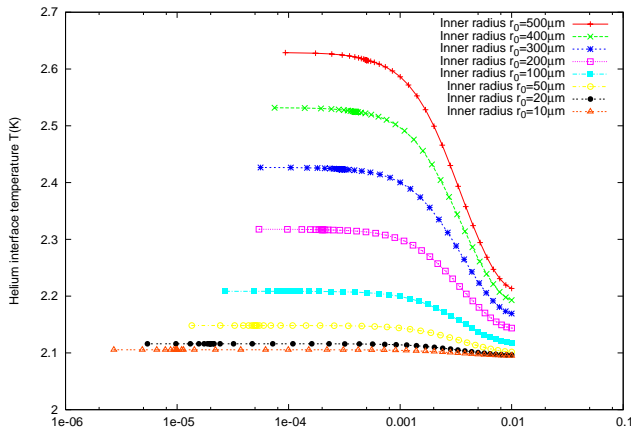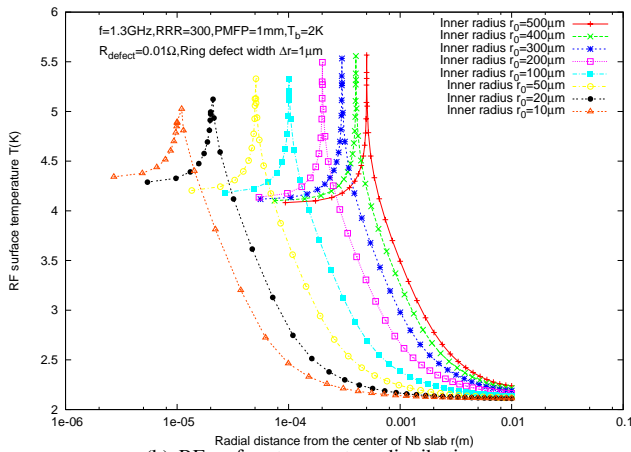

Figure 6: rf surface temperature distribution of a 5mm ring-type defect with 1μm width. The modeled niobium plate has a radius of 10mm.

05 Cavity performance limiting mechanisms

CALCULATION RESULTS

Simulations on ring-shaped defects of different radius and width were performed to explore the relationship between the pre-quench (a steady state with cavity maximum surface magnetic fields just below the quench field) temperature distributions and ring geometries. Figure 7 shows a typical pre-quench temperature distribution along the radial direction both in the helium side and in the rf surface for different inner radius ring-type defect with the same ring width of $1\mu m$. The defect resistance was assumed as $10m\Omega$. The results show a clear dependence of helium side pre-quench temperature on the inner radius of the ring-shaped defect which was similarly discovered in the previous study of the disk-type defect model [2].

(a) Helium side surface temperature distribution.

(b) RF surface temperature distributions.

Figure 7: Temperature distributions for different sizes of ring-type defects with the same ring width of $1\mu m$.

Figure 8 shows the calculated quench field distribution as function of the ring-type defect inner radius for two ring width $1\mu m$ and $2\mu m$. For a pit quenched at 1200Oe as observed in figure 1, a ring width around $1.8\mu m$ can be concluded. Direct measurements by contact profilometry confirmed that the edge of the pit shown in figure 1 was $1\sim2\mu m$. Considering the unincluded magnetic field en-

05 Cavity performance limiting mechanisms

hancement factor at the edge of the pit, the agreement of pit width information between simulated and measured results is acceptable. Combined with thermometry data of quench field H_{quench} and pre-quench helium side temperature reading ΔT, the simulation results of quench field of a ring defect size with the measured pit radius R by profilometry or optical inspections can provide estimates of the resistance of the normal conducting region of the pit as well as of the width of the edge of the pit with strong magnetic field enhancement.
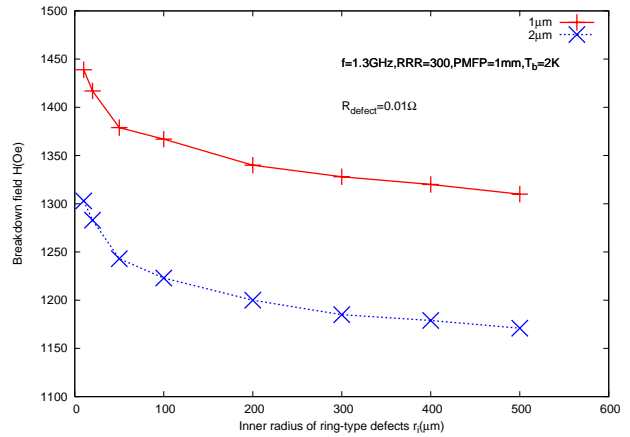

Figure 8: Quench fields v.s. difference ring-type defect sizes for two difference ring width.

CONCLUSION AND FUTURE WORK

A 2-d ring-type defect thermal model has been developed and is benchmarked. This model assumes an ideal ring-shape defect at the edge of pit structures and can provide information on normal conducting resistance and width of normal conducting pit edge. Since both optical and profilometry studies suggests an irregular ring width structure, only a fraction of the ring may go normal conducting. Therefore the calculation results may need a geometrical correction factor depending on the actual pits geometry. Also the magnetic field enhancement factor β which is determined by slopes of ring edges should be considered in the future improved version of thermal ring defect model.

REFERENCES

[1] Y. Iwashita et.al., *"Developement of high resolution camera and observations of superconducting cavities"*, EPAC08, Genoa, Italy.

[2] Y. Xie et.al., *"Possible relationship between defects preheating and defects size"*, SRF09, Berlin, Germany.

[3] V. Shemelin, H. Padamsee, *"Magnetic eld enhancement at pits and bumps on the surface of superconducting cavities"*, SRF Report 080903-04, Cornell University.